AGU PUBLICATIONS

Radio Science

RESEARCH ARTICLE
10.1002/2015RS005890

Special Section:
Ionospheric Effects Symposium 2015

This article is a companion to *Nickisch et al.* [2016] doi:10.1002/2015RS005902.

Key Points:
- Assimilative model for ionosphere employing data from HF channels
- Raypath response operator is introduced
- Consistency of the model with various kinds of input HF data is verified

Correspondence to:
S. V. Fridman,
sergey@nwra.com

Citation:
Fridman, S. V., L. J. Nickisch, M. Hausman, and G. Zunich (2016), Assimilative model for ionospheric dynamics employing delay, Doppler, and direction of arrival measurements from multiple HF channels, *Radio Sci.*, *51*, doi:10.1002/2015RS005890.

Received 1 DEC 2015
Accepted 2 FEB 2016
Accepted article online 5 FEB 2016

Assimilative model for ionospheric dynamics employing delay, Doppler, and direction of arrival measurements from multiple HF channels

Sergey V. Fridman[1], L. J. Nickisch[1], Mark Hausman[1], and George Zunich[2]

[1]NorthWest Research Associates, Monterey, California, USA, [2]Zunicalc, Inc., Monterey, California, USA

Abstract We describe the development of new HF data assimilation capabilities for our ionospheric inversion algorithm called GPSII (GPS Ionospheric Inversion). Previously existing capabilities of this algorithm included assimilation of GPS total electron content data as well as assimilation of backscatter ionograms. In the present effort we concentrated on developing assimilation tools for data related to HF propagation channels. Measurements of propagation delay, angle of arrival, and the ionosphere-induced Doppler from any number of known propagation links can now be utilized by GPSII. The resulting ionospheric model is consistent with all assimilated measurements. This means that ray tracing simulations of the assimilated propagation links are guaranteed to be in agreement with measured data within the errors of measurement. The key theoretical element for assimilating HF data is the raypath response operator (RPRO) which describes response of raypath parameters to infinitesimal variations of electron density in the ionosphere. We construct the RPRO out of the fundamental solution of linearized ray tracing equations for a dynamic magnetoactive plasma. We demonstrate performance and internal consistency of the algorithm using propagation delay data from multiple oblique ionograms (courtesy of Defence Science and Technology Organisation, Australia) as well as with time series of near-vertical incidence sky wave data (courtesy of the Intelligence Advanced Research Projects Activity HFGeo Program Government team). In all cases GPSII produces electron density distributions which are smooth in space and in time. We simulate the assimilated propagation links by performing ray tracing through GPSII-produced ionosphere and observe that simulated data are indeed in agreement with assimilated measurements.

1. Introduction

HF sky wave propagation channels are known to be greatly influenced by ionospheric variations. These variations manifest themselves in HF measurements as fluctuations of the propagation delay, angles of arrival, and the ionosphere-induced shift of signal frequency (ionospheric Doppler). This sort of data carries information about spatial and temporal structure of the electron density in the ionosphere, albeit in a convoluted, implicit way. We have developed a formulation for recovering equivalent ionospheric structures from measurements of HF probes.

This problem of inverting HF data is approached as the task of extending capabilities of GPSII—the assimilative model of the ionosphere described in *Fridman et al.* [2006, 2012]. GPSII is capable of ingesting data from GPS and low Earth orbiting satellite beacons, in situ electron density, vertical incidence sounders, and leading edges of backscatter ionograms to derive a three-dimensional ionosphere model that is both spatially and temporally smooth but is yet in agreement with all the input data to within the data measurement error.

In the next section we will describe our formulation for incorporating HF data into ionospheric inversions followed by illustrations of algorithm operation. The companion paper by *Nickisch et al.* [2016] in this issue offers quantitative analysis of the algorithm performance for one data collection campaign.

2. Merging HF Data With GPSII

Our approach to solving the ionospheric inverse problem is inherited from the GPSII algorithm [*Fridman et al.*, 2006, 2012]. We represent the three-dimensional, time-varying distribution of electron density in the ionosphere as

$$n(\mathbf{r},t) = n_0(\mathbf{r},t)Q[u(\mathbf{r},t)] \quad (1)$$

where $n_0(\mathbf{r}, t)$ is a background model of the ionosphere, $Q(s)$ is a user-defined monotonically increasing function of one variable such that $Q(-\infty) = 0$, $Q(\infty) = \infty$, and $u(\mathbf{r}, t)$ is an arbitrary function which will be determined as a result of the inversion procedure. Results presented in this paper employ IRI-2007 as the background model. The function $Q(s)$ is selected in the following form:

$$Q(s) = \begin{cases} e^s\,, & s \le 0 \\ 1 + s + 0.5s^2 - s^3/3\,, & 0 < s \le 0.5 \\ 1.25s + 23/24\,, & s > 0.5 \end{cases} \tag{2}$$

This function is continuous along with its first and second derivatives, it decays exponentially at negative s, and it behaves linearly at large positive s.

The numerical solution will be performed over a four-dimensional spatial-temporal grid. The vector of values of $u(\mathbf{r}, t)$ in all nodes of this grid will be denoted U (we are using boldface only for vectors in three-dimensional physical space). The unknown vector U is related to the vector of available measured quantities Y:

$$Y = M[U] + \eta. \tag{3}$$

Here M is the measurement operator. It is a known nonlinear operator that relates the ionospheric model (which is specified by U) to theoretical estimates of each of the measured quantities, and vector η represents the noise of measurements. It is assumed that the noise covariance matrix of measurement errors is known.

The task of the ionospheric inverse problem is to resolve equation (3) with respect to U. In order to solve it within the GPSII framework, it is necessary to provide L—the linearized version of the measurement operator M: $L = \delta M[U]/\delta u$. Once procedures for calculating the vector $M[U]$ and the linear operator L are in place, the unknown vector of ionospheric modification U may be found iteratively using Tikhonov's regularization technique with the residual principle as described in section 2.2 of *Fridman et al*. [2006]. This inversion technique takes into account the statistics of errors of measurements and ensures that diverse data types are ingested simultaneously and with proper weights.

Thus, in order to incorporate the HF channel probe data into GPSII, we need to provide means for calculating the theoretical channel probe data for any ionosphere represented by (1). This will augment $M[U]$ with the components representing the HF data $M_{\mathrm{HF}}[U]$. We also need to augment L with $L_{\mathrm{HF}} = \delta M_{\mathrm{HF}}[U]/\delta u$ which is the linearization of M_{HF}. Both tasks are solved with the aid of numerical ray tracing as outlined below.

2.1. Extended Ray Tracing Equations

We employ Hamiltonian formulation of the ray tracing (RT) equations [*Haselgrove*, 1957; *Jones and Stephenson*, 1975]:

$$\frac{\mathrm{d}\mathbf{R}}{\mathrm{d}\tau} = -\frac{\partial H}{\partial \mathbf{k}} \Big/ \frac{\partial H}{\partial \omega}, \qquad \frac{\mathrm{d}\mathbf{k}}{\mathrm{d}\tau} = \frac{\partial H}{\partial \mathbf{R}} \Big/ \frac{\partial H}{\partial \omega}, \qquad \frac{\mathrm{d}\omega}{\mathrm{d}\tau} = -\frac{\partial H}{\partial t} \Big/ \frac{\partial H}{\partial \omega} \tag{4}$$

where τ is the group delay, $\mathbf{R}(\tau)$ is the position of the wave packet in space, $\mathbf{k}(\tau)$ is the wave vector, and $H(\mathbf{R}, \mathbf{k}, \omega, t)$ is the RT Hamiltonian. Initial values of solution components $[\mathbf{R}, \mathbf{k}, \omega]\big|_{\tau = 0}$ must satisfy the dispersion relation $H(\mathbf{R}, \mathbf{k}, \omega, t) = 0$.

The Hamiltonian may be in any form discussed by *Jones and Stephenson* [1975]. The default form of the Hamiltonian in GPSII is

$$H = \frac{\omega}{2}\left[\left(\frac{ck}{\omega}\right)^2 - \mu^2\right] \tag{5}$$

where $\mu(\mathbf{k}, \mathbf{R})$ is the refractive index of cold, collision-free plasma as presented in *Davies* [1990, expression (3.9)].

In order to simplify derivations, we are going to use Cartesian coordinates throughout this paper. Transformation to the Earth-centered spherical coordinates that are employed in our practical codes is straightforward.

It is convenient to rewrite equation (4) as a single equation for the seven-component solution vector $X = [\mathbf{R}, \mathbf{k}, \omega]^T$:

$$\frac{\mathrm{d}}{\mathrm{d}\tau} X = F\left(X, \left[n, \frac{\partial n}{\partial t}\right]\right) \tag{6}$$

We explicitly show here that the right-hand side above depends on spatial fields of electron density and the time derivative of electron density.

In order to construct L_{HF}, we augment the RT equations with their linearized version:

$$\frac{\mathrm{d}}{\mathrm{d}\tau}A = BA \tag{7}$$

where the seven-element columns of matrix $A(\tau)$ represent linearized solutions of the system and B is a 7 by 7 matrix whose elements $b_{ij} = \partial f_i/\partial x_j$ are

$$\begin{aligned}
b_{1:3,1:3} &= \left[-\frac{\partial}{\partial \mathbf{R}}\otimes\frac{\partial H}{\partial \mathbf{k}}\Big/\frac{\partial H}{\partial \omega}\right]^T, \quad b_{1:3,4:6} = \left[-\frac{\partial}{\partial \mathbf{k}}\otimes\frac{\partial H}{\partial \mathbf{k}}\Big/\frac{\partial H}{\partial \omega}\right]^T, \quad b_{1:3,7} = -\frac{\partial}{\partial \omega}\frac{\partial H}{\partial \mathbf{k}}\Big/\frac{\partial H}{\partial \omega} \\
b_{4:6,1:3} &= \left[\frac{\partial}{\partial \mathbf{R}}\otimes\frac{\partial H}{\partial \mathbf{R}}\Big/\frac{\partial H}{\partial \omega}\right]^T, \quad b_{4:6,4:6} = \left[\frac{\partial}{\partial \mathbf{k}}\otimes\frac{\partial H}{\partial \mathbf{R}}\Big/\frac{\partial H}{\partial \omega}\right]^T, \quad b_{4:6,7} = \frac{\partial}{\partial \omega}\frac{\partial H}{\partial \mathbf{R}}\Big/\frac{\partial H}{\partial \omega} \\
b_{7,1:3} &= -\frac{\partial}{\partial \mathbf{R}}\frac{\partial H}{\partial t}\Big/\frac{\partial H}{\partial \omega}, \quad b_{7,4:6} = -\frac{\partial}{\partial \mathbf{k}}\frac{\partial H}{\partial t}\Big/\frac{\partial H}{\partial \omega}, \quad b_{7,7} = -\frac{\partial}{\partial \omega}\frac{\partial H}{\partial t}\Big/\frac{\partial H}{\partial \omega}
\end{aligned} \tag{8}$$

In our algorithm the extended system of RT equations (6) and (7) is solved numerically for the 7 by 7 matrix $A(\tau)$ subject to the initial condition $A(0) = I$, where I is the identity matrix. Thus, columns of $A(\tau)$ comprise the fundamental solution of (7).

2.2. Raypath Response Operator

For a given receiver-transmitter configuration of a channel probe and for a given distribution of electron density $n(\mathbf{r}, t)$ one can find rays that connect receiver and transmitter [*Coleman*, 2011] in accordance with the RT equations. Then theoretical values for probe's measurements at the receive site (such as propagation delay, angles of arrival, and ionosphere-induced Doppler shift) can be expressed in terms of components of the vector $J(t) = [\tau_L, \mathbf{k}_L, \omega_L]$, where τ_L is the value of τ at the landing point of the traced ray, $\mathbf{k}_L = \mathbf{k}(\tau_L)$, and $\omega = \omega(\tau_L)$.

The following is the definition of the raypath response operator (RPRO). The RPRO relates infinitesimal variations of $n(\mathbf{r}, t)$ at the time instant t to variation of components of the vector J:

$$\delta J = \iiint\left[R^S(\mathbf{r})\delta n + R^D(\mathbf{r})\delta\left(\frac{\partial}{\partial t}n\right)\right]\mathrm{d}^3\mathbf{r} \tag{9}$$

Here R^S and R^D are static and dynamic components of the RPRO.

The relationship between L_{HF} and RPRO is straightforward (as is illustrated at the end of this section), so we will concentrate on deriving components of the RPRO. The plan is to construct a Green function for the linear equation (7). This will allow us to relate perturbation of the RT solution to infinitesimal variations of the right-hand side in (6). The variations of the later can be directly related to perturbations of electron density.

Assuming that the matrix $A(\tau)$ is available as a result of numerical ray tracing, the Green function (the impulse response function) for (7) regarded as the initial value problem is

$$G^I(\tau, \tau') = \begin{cases} 0, \tau \le \tau' \\ A(\tau)A^{-1}(\tau'), \tau > \tau' \end{cases} \tag{10}$$

Indeed, this function satisfies the impulse response equation for the linearized system

$$\frac{\mathrm{d}}{\mathrm{d}\tau}G = BG + I\delta(\tau - \tau') \tag{11}$$

subject to zero initial conditions ($G^I|_{\tau=0} = 0$). What we actually need is the Green function $G(\tau, \tau')$ (that is, the solution to equation (11)) for the boundary value problem where end points of perturbed rays remain fixed [*Afanasyev et al.*, 1982]. In this case the starting wave vector $\mathbf{k}_S$ and the group delay at landing τ_L are affected by perturbations along the ray. Denoting the unknown response of $\mathbf{k}_S$ as $K(\tau')$ (this is a 3×7 matrix related to the yet unknown Green function as $K(\tau') = G(0, \tau')_{[4:6,1:7]}$) and the response of τ_L as $T(\tau')$ (this is a 1×7 matrix), we can express the Green function of the point-to-point ray perturbation problem as

$$G(\tau, \tau') = G^I(\tau, \tau') + G^I(\tau, 0)_{[1:7,4:6]}K(\tau')_{[1:3,1:7]} \tag{12}$$

The second term in this expression introduces raypath perturbations associated with perturbations of the starting wave vector while position of the starting point remains unperturbed. The response functions $K(\tau')$ and $T(\tau')$ are determined from the requirement that the perturbation in spatial position of the landing point is zero:

$$G^I(\tau_L,\tau')_{[1:3,1:7]} + G^I(\tau_L,0)_{[1:3,4:6]}K(\tau')_{[1:3,1:7]} + \dot{X}(\tau_L)_{[1:3]}T(\tau')_{[1,1:7]} = 0$$
$$\dot{X}(0)_{[1:3]}^{T}K(\tau') = 0 \tag{13}$$

Here $\dot{X} = \mathrm{d}X/\mathrm{d}\tau$, found within the unperturbed RT problem. The second equation above reflects the requirement that the dispersion relation $H(\mathbf{R},\mathbf{k},\omega,t) = 0$ remains fulfilled by the perturbed starting wave vector (we exploited the first equation in (4) to express this requirement in a simpler form). Solving the matrix equation (13) with respect to $K(\tau')$ and $T(\tau')$, we find

$$\begin{bmatrix} K(\tau') \\ T(\tau') \end{bmatrix} = \begin{bmatrix} G^I(\tau_L,0)_{[1:3,4:6]} & \dot{X}(\tau_L)_{[1:3,1]} \\ \dot{X}(0)_{[1,1:3]}^{T} & 0 \end{bmatrix}^{-1} \begin{bmatrix} G^I(\tau_L,\tau')_{[1:3,1:7]} \\ 0 \end{bmatrix} \tag{14}$$

Upon substituting $K(\tau')$ into (12), we obtain the impulse response of state vector X as a function of the propagation delay τ from the ray starting point. The response function for the state vector at the location of the receiver is

$$G^L(\tau') = G^I(\tau_L,\tau') + G^I(\tau_L,0)_{[1:7,4:6]}K(\tau') + \dot{X}(\tau_L)_{[1:7,1]}T(\tau')_{[1,1:7]} \tag{15}$$

The last term in the above expression accounts for the perturbation of the propagation delay.

The components of the RPRO may be expressed in terms of the impulse response functions G^L and T:

$$R^S(\mathbf{r}) = \int_0^{\tau_L} \begin{bmatrix} T(\tau)_{[1,1:7]} \\ G^L(\tau)_{[4:7,1:7]} \end{bmatrix} \frac{\delta F(X(\tau),[n,\partial n/\partial t])}{\delta n} d\tau \tag{16}$$

$$R^D(\mathbf{r}) = \int_0^{\tau_L} \begin{bmatrix} T(\tau)_{[1,1:7]} \\ G^L(\tau)_{[4:7,1:7]} \end{bmatrix} \frac{\delta F(X(\tau),[n,\partial n/\partial t])}{\delta(\partial n/\partial t)} d\tau \tag{17}$$

In these expressions the functional derivatives are evaluated assuming that n and $\partial n/\partial t$ are independent fields. The following two properties of functional derivatives should be kept in mind when evaluating $\delta F/\delta n$ in (16) and (17). Suppose that a functional $\varphi[n]$ amounts to a simple function ($\varphi[n] \equiv \varphi(n(\mathbf{r}))$). Then $\frac{\delta\varphi}{\delta n} = \varphi'(n(\mathbf{r}))\delta(\mathbf{r}-\mathbf{r}')$, where $\delta(\mathbf{r}-\mathbf{r}')$ is the delta function in three-dimensional space and $\varphi'(n) = \partial\varphi(n)/\partial n$. The following property is useful for handling terms in the ray tracing equations that contain spatial derivatives of electron density: $\frac{\delta}{\delta n}\frac{\partial n}{\partial \mathbf{r}} = \frac{\partial}{\partial \mathbf{r}}\delta(\mathbf{r}-\mathbf{r}')$.

It is justified to set $R^D_{[1:4]} = 0$ because relative magnitude of the Doppler shift of operating frequency is negligibly small for ionospheric propagation paths. The only nonnegligible component of R^D is the Doppler shift component which can be rewritten as follows:

$$R^D(\mathbf{r})_{[5]} = -\int_0^{\tau_L} G^L(\tau)_{[7,7]} \frac{H_n(\mathbf{R}(\tau),\mathbf{k}(\tau),\omega_0)}{\partial H(\mathbf{R}(\tau),\mathbf{k}(\tau),\omega_0)/\partial\omega_0} \delta(\mathbf{r}-\mathbf{R}(\tau))\mathrm{d}\tau \tag{18}$$

Here ω_0 is the frequency of the transmitted signal and $H_n = \partial H/\partial n$. The later expression is formulated with the understanding that the Hamiltonian depends on the temporal coordinate entirely via its dependence on $n(\mathbf{r},t)$; that is, $H(\mathbf{r},\mathbf{k},\omega,t) = H(n(\mathbf{r},t),\mathbf{k},\omega)$.

As an example, consider transformation of RPRO into L_{HF} for the case of a single Doppler measurement (assume radian per second units) over a single propagation path. Formally,

$$L_{\mathrm{HF}} = n_0(\mathbf{r},t)Q'[u(\mathbf{r},t)]\left[R^S\delta(\bar{t}-t) + R^D\delta'(\bar{t}-t)\right] \tag{19}$$

where $\bar{t}$ is the time instant of the measurement, $Q'(s) = \mathrm{d}Q(s)/\mathrm{d}s$, and $\delta'(s) = \mathrm{d}\delta(s)/\mathrm{d}s$. The operator L_{HF} needs to be approximated over the spatial-temporal grid of the solution. For this purpose delta function operators are replaced with appropriate interpolation over the grid operators, and the integral in (18) is approximated by a finite sum as it is described in Appendix A.

3. GPSII Operation With Channel Probe Data

Data from a network of near-vertical propagation channels were provided to us by the Intelligence Advanced Research Projects Activity (IARPA) HFGeo Program. Figure 1 shows locations of the receiver and five

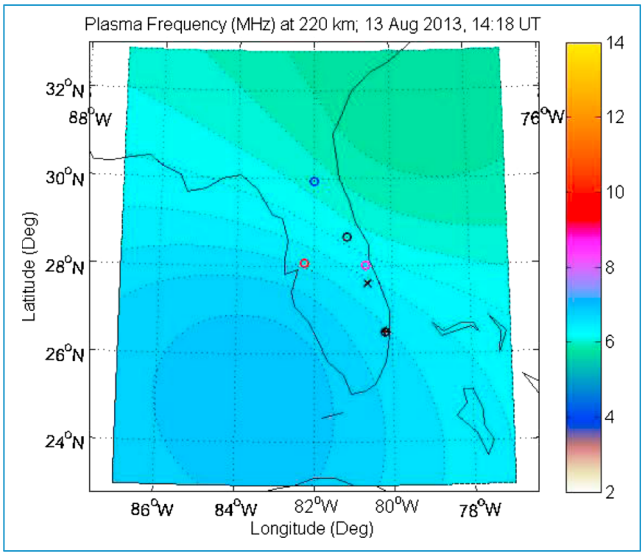

Figure 1. HF transmitters (circles) and receiver (crosses) providing range-Doppler data over five propagation channels. The contour plot presents the horizontal cross section (220 km altitude) of one frame (1418 UT, 13 August 2013) of the GPSII solution driven by the HF data from the five transmitters.

transmitters operated in Florida. An example of range-Doppler time series collected on one of the links is shown in Figure 2. (Note that the use of the term "range" here refers to "slant range" or group path length, that is, delay times the speed of light.) GPSII inversion was performed using only HF data from all links with a time cadence of 1 min; time step of the solution was set to 1 min as well. Correlation-scale parameters of the pseudocovariance matrix [*Fridman et al.*, 2006] were set to the value of 1° for both horizontal directions, while the vertical scale varied from about 25 km at the bottom boundary of the domain (altitude of 80 km) to about 200 km at the top boundary (1000 km). Solution grid size was approximately 0.1° in both horizontal dimensions, while the altitude step size varied from about 0.3 km to 20 km. The contour plot in Figure 1 shows a snapshot of the horizontal cross section of the solution at altitude 220 km (approximate altitude of reflection of the rays). One can see that the solution remains quite smooth while the ionosphere is modified to match the data. The GPSII fit to the data as reported by the internal ray tracing is also shown in Figure 2. The GPSII-derived prediction follows data quite closely during most of the analyzed time interval. Statistical analysis of GPSII performance for these kinds of data is provided in the companion paper by *Nickisch et al.* [2016].

A valuable data set from a network of oblique ionogram (OI) links and vertical sounders was provided to us by Defence Science and Technology Organisation (DSTO) (Australia). Figure 3 illustrates the configuration of the OI links, vertical sounders, and GPS receivers that were employed in one of our tests. These selected links are a small subset of dozens OI paths monitored by DSTO. OI data were provided to GPSII as a number of delay-frequency samples for the extraordinary (*X*) mode for each participating OI link. An example of data samples collected from one of the OIs (ASP-SCH link) is indicated by boxes in Figure 4 (left). The GPSII solution was produced with a cadence of 15 min. GPS total electron content (TEC) data were sampled with 15 min time interval. OI and VI data were occasionally decimated to ensure that any given OI or VI contributes only once per solution time step. Correlation-scale parameters of the pseudocovariance matrix were set to 5° for both horizontal dimensions. The altitude-dependent vertical correlation scale varied from about 25 km at the

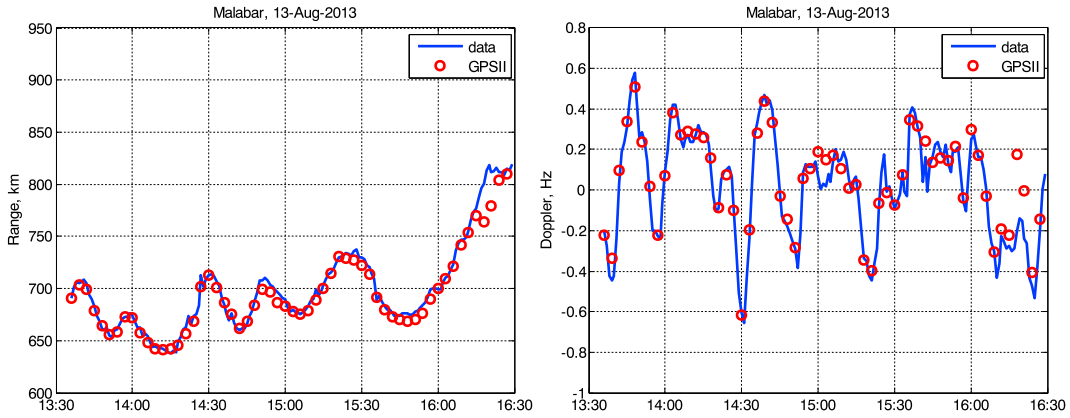

Figure 2. Example of (left) range and (right) Doppler data compared to GPSII fit (circles).

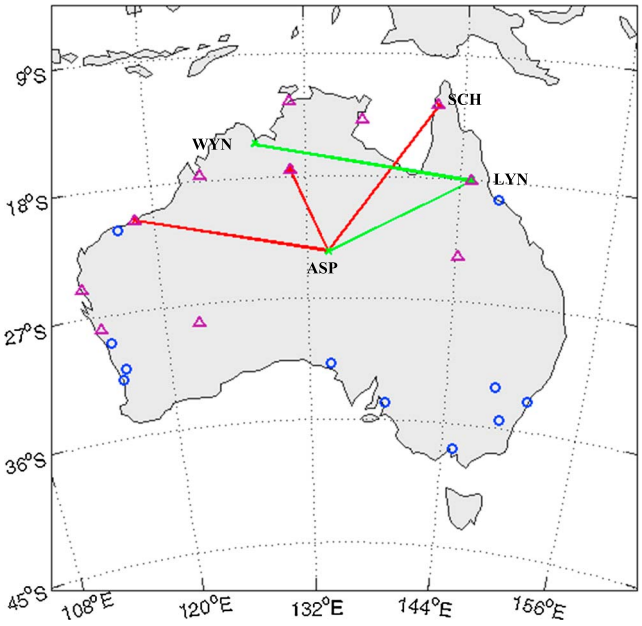

Figure 3. Assimilated OI links (red segments), assimilated vertical profiles (triangles), and GPS TEC receivers along with the test OI link (WYN-LYN).

bottom boundary of the domain (altitude of 80 km) to about 1000 km at the top boundary (20000 km). The solution grid size was approximately 0.5° in both horizontal dimensions, while the altitude step size varied from about 0.3 km to 200 km.

Synthetic OIs were generated by ray tracing through GPSII ionosphere using an external numerical ray tracing code. A good match to the observed OI trace is evident in Figure 4 when OI data are assimilated (yellow points). It is notable that the same GPSII model provides good agreement for the nonassimilated OI link (WYN-LYN). Figure 4 also illustrates that the ionospheric model obtained without any OI data assimilated (red points) fails to provide satisfactory agreement with the OI data. (Note that GPS L1/L2 beacon data and vertical ionograms were assimilated in all cases. We also note that the ionosphere was exceptionally dynamic at this time due to large-scale traveling ionospheric disturbance activity.) Figure 5 shows comparison of zonal distributions of plasma obtained with and without OI data for the time of observations in Figure 4. Figure 5 (bottom) represents inversion without OI data. One can note prominent zonal modulation of the

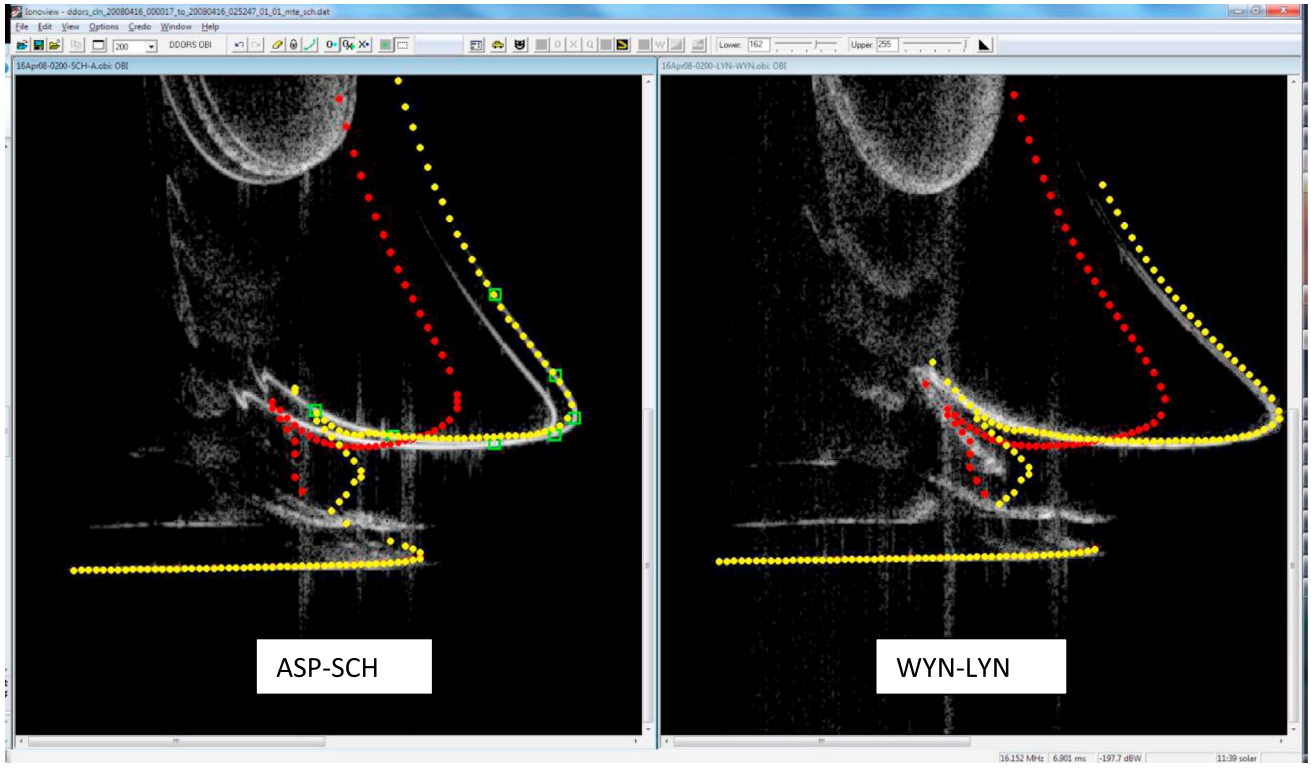

Figure 4. OIs collected on 16 April 2008, 0202 UT, compared to *X*-mode synthetic traces (yellow dots). (left) One of the assimilated data links. Frequency-delay data supplied to GPSII are marked by green boxes. (right) Data from a validation (nonassimilated) link. Red dots show synthetic OIs for a different GPSII solution that was obtained without assimilating OI data (only GPS and VI data were assimilated in this case).

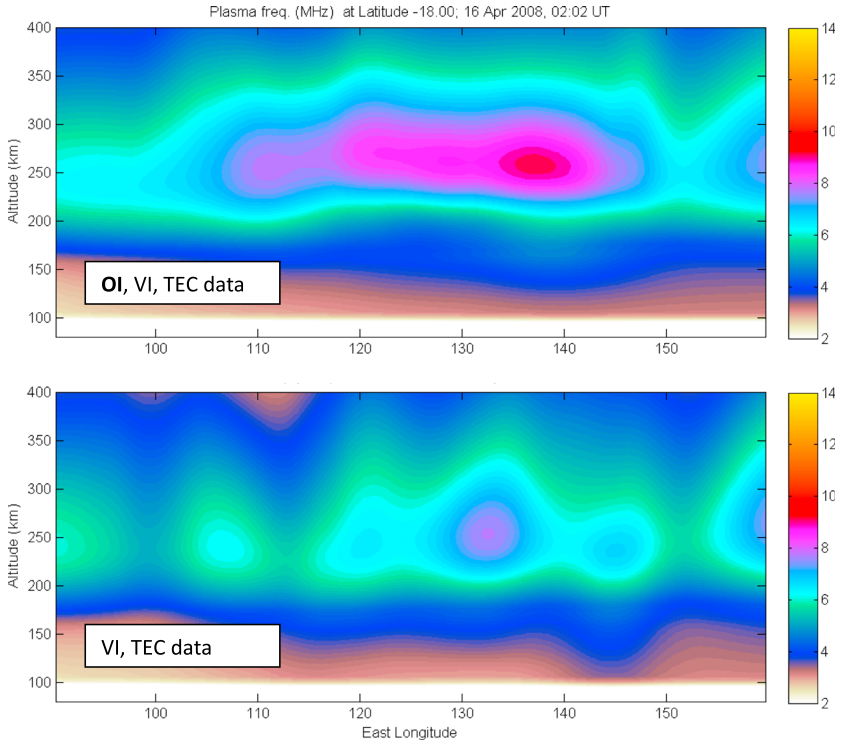

Figure 5. Vertical cross section of GPSII solutions at a constant latitude of 18° south. (top) Solution driven by OI, VI, and GPS TEC data compared to the (bottom) solution driven by VI and GPS TEC.

solution that may be attributed to the impact of data from nearby VI sounders (at longitudes 118.6, 123.8, 130.8, and 144.9°) as well as impact from the line of sight of one of the GPS receivers. The scale of this modulation is consistent with the adopted solution correlation scale of 5°. This modulation effect becomes less prominent with the addition of OI data (Figure 5, top). It appears that OI data that probe geographically extended volumes of the ionosphere help to smoothly connect localized effects of sparse VI sounders and GPS receivers.

4. Conclusions

We have developed theoretical framework for incorporating HF channel probe data (propagation delay, angles of arrival, and Doppler shift) into ionospheric inversion algorithms. We have extended capabilities of GPSII (our ionospheric inversion algorithm) to incorporate data from HF channel probes and oblique ionograms. Performance of the new algorithm was demonstrated using range-Doppler time series produced by a network of short-range HF channel probes. In another demonstration we operated the algorithm with data from a network of OI sounders. We performed ray tracing through the GPSII-produced ionosphere using an independent numerical ray tracing code and observed that simulated data are indeed in agreement with assimilated measurements.

Appendix A: Numerical Approximation of Delta Function Operators and Matrix Representation of L_{HF}

The one-dimensional delta function operator is defined by requiring that the following relationship is valid for an arbitrary continuous function $f(s)$:

$$\int_{-\infty}^{\infty}\delta(s-p)f(s)\mathrm{d}s = f(p) \tag{A1}$$

Assuming that the function $f(s)$ is specified by a vector of its values $f_i = f(s_i)$ in nodes s_i, the operator (A1) may be approximated by the sum

$$\int_{-\infty}^{\infty}\delta(s-p)f(s)\mathrm{d}s \approx \sum_i \left(\delta_{i,m}\frac{s_{m+1}-p}{s_{m+1}-s_m} + \delta_{i,m+1}\frac{p-s_m}{s_{m+1}-s_m}\right)f_i \tag{A2}$$

Where $\delta_{i,m}$ is the Kroneker delta, $m = m(p)$ specifies the interval that contains point p, and $m : s_m \le p < s_{m+1}$. It is easy to see that (A2) provides the linear interpolation approximation to $f(p)$. A sampled approximation to the operator $\delta'(s-p)$ is obtained by differentiating (A2) with respect to p:

$$\int_{-\infty}^{\infty} \delta'(s-p) f(s) \mathrm{d}s \approx \sum_i \frac{\delta_{i,m} - \delta_{i,m+1}}{s_{m+1} - s_m} f_i \tag{A3}$$

Multidimensional delta function operators and their first derivatives are obtained by applying transformations (A2) and (A3) to each of the spatial-temporal dimensions. In order to illustrate this procedure, we will proceed with the example of a single Doppler measurement that resulted in the expression (18) for RPRO. Substitute (18) into (19) (keep in mind that $R^S = 0$ in this case), change order of integration operations, approximate integration over τ (along the raypath) by a sum over variable l using the trapezoid formula, and exploit approximations (A2) and (A3). We obtain

$$\begin{aligned} &\int_{t_N}^{t_{N+1}} \mathrm{d}t' \iiint \mathrm{d}\mathbf{r} L_{HF}(\mathbf{r}, t') \delta u(\mathbf{r}, t') \approx \\ &\sum_l D_l \sum_{p=0}^{1} \sum_{h=0}^{1} \sum_{g=0}^{1} \sum_{e=0}^{1} n_0\left(x_{i_l+h}, y_{j_l+g}, z_{k_l+e}, t_{N+p}\right) Q'\left[u\left(x_{i_l+h}, y_{j_l+g}, z_{k_l+e}, t_{N+p}\right)\right] (-1)^{p+1} \\ &\frac{|x_{i_l+1-h} - R_x(l)|}{x_{i_l+1} - x_{i_l}} \frac{\left|y_{j_l+1-g} - R_y(l)\right|}{y_{j_l+1} - y_{j_l}} \frac{|z_{k_l+1-e} - R_z(l)|}{z_{k_l+1} - z_{k_l}} \delta u(i_l + h, j_l + g, k_l + e, N + p) \end{aligned} \tag{A4}$$

Here $[t_N, t_{N+1}]$ is the solution time interval that contains the time instant $\bar{t}$ of the measurement, $[R_x(l), R_y(l), R_z(l)]^T = \mathbf{R}(\tau_l)$, and (i_l, j_l, k_l) specifies position of the voxel of three-dimensional grid of the spatial variable $\mathbf{r} = [x, y, z]^T$ that contains the point $\mathbf{R}(\tau_l)$, so that

$$x_{i_l} \le R_x(l) < x_{i_l+1}, \quad y_{j_l} \le R_y(l) < y_{j_l+1}, \quad z_{k_l} \le R_z(l) < z_{k_l+1} \tag{A5}$$

$$D_l = -G^L(\tau_l)_{[7,7]} \frac{H_n(\mathbf{R}(\tau_l), \mathbf{k}(\tau_l), \omega_0)}{\partial H(\mathbf{R}(\tau_l), \mathbf{k}(\tau_l), \omega_0)/\partial \omega_0} \frac{\tau_{l+1} - \tau_{l-1}}{2} \frac{1}{t_{N+1} - t_N} \tag{A6}$$

Expression (A4) provides the desired matrix representation of the operator L_{HF}. This matrix specifies linear response of measured Doppler to variations of the function u in nodes of the four-dimensional grid of the solution.

Acknowledgments

This research is based upon work supported in part by the Office of the Director of National Intelligence (ODNI) Intelligence Advanced Research Projects Activity (IARPA) HFGeo program under contract 2013-13082600004 and in part by the Air Force Research Laboratory under contract FA9453-11-C-0157. The views and conclusions contained herein are those of the authors and should not be interpreted as necessarily representing the official policies or endorsements, either expressed or implied, of ODNI, IARPA, AFRL, or the U.S. Government. The U.S. Government is authorized to reproduce and distribute reprints for governmental purposes notwithstanding any copyright annotation thereon. The vertical and oblique ionogram data utilized in section 5 of this paper were provided by the Australian Defence Science and Technology Organisation (DSTO).

References

Afanasyev, N. T., S. M. Mikheev, and M. V. Tinin (1982), Some results of applying the perturbation technique to the two-point trajectory problem, in *Simulation of Ionospheric Processes and Propagation of Radio Waves*, pp. 124–134, ISU, Irkutsk, (in Russian).

Coleman, C. J. (2011), Point-to-point ionospheric ray tracing by a direct variational method, *Radio Sci.*, *46*, RS5016, doi:10.1029/2011RS004748.

Davies, K. (1990), *Ionospheric Radio*, Peter Peregrinus Ltd., London, U. K.

Fridman, S. V., L. J. Nickisch, M. Aiello, and M. A. Hausman (2006), Real time reconstruction of the three-dimensional ionosphere using data from a network of GPS receivers, *Radio Sci.*, *41*, RS5S12, doi:10.1029/2005RS003341.

Fridman, S. V., L. J. Nickisch, and M. Hausman (2012), Inversion of backscatter ionograms and TEC data for over-the-horizon radar, *Radio Sci.*, *47*, RS0L10, doi:10.1029/2011RS004932.

Haselgrove, J. (1957), Oblique ray paths in the ionosphere, *Proc. Phys. Soc. London, Sect. B*, *70*, 653.

Jones, R. M., and J. J. Stephenson (1975), A versatile three-dimensional ray tracing computer program for radio waves in the ionosphere, OT Rep., 75-76, U. S. Department of Commerce, Office of Telecommunication, U. S. Government Printing Office, Washington, USA, 185 pp.

Nickisch, L. J., S. Fridman, M. Hausman, S. Kraut, and G. Zunich (2016), Assimilative modeling of ionospheric dynamics for nowcasting of HF propagation channels in the presence of TIDs, *Radio Sci.*, *51*, doi:10.1002/2015RS005902.